

**Exciton-polariton dynamics in a transparent organic semiconductor microcavity**

Jung-Hoon Song,\* Y. He, and A. V. Nurmikko

*Division of Engineering and Department of Physics, Brown University, Providence, Rhode Island 02912, USA*

J. Tischler and V. Bulovic

*Department of Electrical Engineering and Computer Science, Massachusetts Institute of Technology, Cambridge, Massachusetts 02139, USA*

(Received 3 July 2003; revised manuscript received 15 December 2003; published 30 June 2004)

Exciton-polariton dynamics are studied in organic semiconductor microcavities operating in the strongly coupled polariton regime, with thin films of cyanine J-aggregates sandwiched between low-loss dielectric mirrors. The delocalized excitons are subject to polariton normal mode splittings which are modulated by near resonant femtosecond excitation pulses, while orientational disorder effects on the formation of polariton states play an important role in polariton dynamics.

DOI: 10.1103/PhysRevB.69.235330

PACS number(s): 71.36.+c, 72.80.Le, 78.47.+p, 82.53.Xa

The linear and nonlinear optical response optical of microcavity polaritons, where excitons in thin semiconductors films are resonantly coupled with cavity photons, has attracted fundamental interest, with possible applications to nonlinear devices.<sup>1,2</sup> Due to their composite particle nature and coherency, cavity polaritons can offer large optical nonlinearities and fast response time, attributes which make them attractive e.g. for prospective high-speed photonic switching.

Polariton-induced enhancement of the nonlinear response and associated dynamics in inorganic semiconductor microcavities has been extensively studied.<sup>3-5</sup> In II-VI and III-V compound semiconductors the normal mode or “Rabi” splittings, which represent the strength of the exciton-photon coupling may reach up to  $\sim 20$  meV in case of II-VI quantum wells at cryogenic temperatures<sup>6</sup> and are smaller in GaAs-based microcavities. Hence such cavity polaritons are not stable at room temperature, in contrast to the case in organic microcavities which show much larger Rabi splittings than their inorganic counterparts.<sup>7,8</sup> Linear aggregates of a cyanine dye have been the organic material of choice in such recent microcavity work where the large Frenkel exciton linewidths associated with the isolated monomer can be significantly narrowed in the aggregates, endowed with giant oscillator strength. Typically organic semiconductor microcavities have been fabricated with a thin metal film as the top mirror, the bottom mirror being also a metal film or a low-loss distributed Bragg reflector (DBR). As a practical matter, it is nontrivial to fabricate dielectric DBRs atop organic materials due to the relatively harsh environment involved in the deposition process. Yet the presence of such transparent reflectors is imperative for low-loss device applications such as in ultrafast optical switching.

In this work, we report on the initial study of room temperature exciton-polaritons based on J-aggregates of cyanine embedded in microcavities with all-dielectric DBRs. We have performed fsec pump-probe experiments on these “transparent” microcavities, to investigate the nonlinear response and the dynamics of the cavity polaritons at room temperature. Recently, subpsec nonlinear response has been demonstrated in J-aggregate cyanine bare thin films with

modulated optical transmission  $\Delta T/T$  order of  $10^{-3}$ .<sup>9</sup> In addition to basic study of the dynamics of strongly coupled excitations in their nonlinear regime, the possibility of achieving optical switching by imbedding medium of such large oscillator strength in a transparent microcavity derives from expected increase in the modulation amplitude, its speed and spectral tailoring. Here we report a strong dependence of both optical nonlinearity and its response time on the coupling strength between the photon and the exciton in the sub-psec regime, with the magnitude of the optical nonlinearity enhanced by more than one order of magnitude by the polariton effect in comparison with bare films.

Our microcavity consists of J-aggregates of cyanine dye layers (2, 2'-dimethyl-8-phenyl-5, 6, 5', 6'-dibenzothiacarbo-cyanine chloride) sandwiched between two dielectric DBR mirrors. A strong and Stoke-shift-free J-band at 690 nm was observed in absorption and emission spectra of a film of the cyanine dye, with peak absorbance ( $\alpha L$ ) of 0.22 and a linewidth of  $\Delta\lambda = 20$  nm. Ion beam sputtering was employed to grow the DBRs, consisting of 7 pairs of SiO<sub>2</sub>/HfO<sub>2</sub> bilayers, each of which is  $\lambda/4n$  thick. Figure 1(a) shows the schematic of the microcavity structure. The organic films were spin-coated atop the bottom DBRs deposited on a glass substrate. The J-aggregates themselves were dispersed in polyvinyl alcohol (PVA) matrix giving film thickness for a  $\lambda/2$  cavity. We then proceeded to use a very low growth rate to deposit the second DBR, 0.02 nm/sec for HfO<sub>2</sub> and 0.04 nm/sec for SiO<sub>2</sub>. The substrate temperature was monitored continuously and kept below 30°C by proper interruptions during the deposition process to maintain the physical and chemical integrity of the organic material. To enable angular tuning, microcavities were fabricated such that the cavity mode was at longer wavelength than the exciton transition at normal incidence, and reached a resonant condition near  $\sim 33^\circ$  angle of incidence. Typical reflectance spectra of DBRs and the transmission spectrum of the full microcavity structure at normal incidence are shown in Figure 1(b), where the peak reflectivity of the DBRs is 0.9, and the cavity mode is located at 720 nm, giving J-aggregate film thickness of 275 nm by fitting for the wavelength location of the cavity mode at normal incident using a transfer matrix

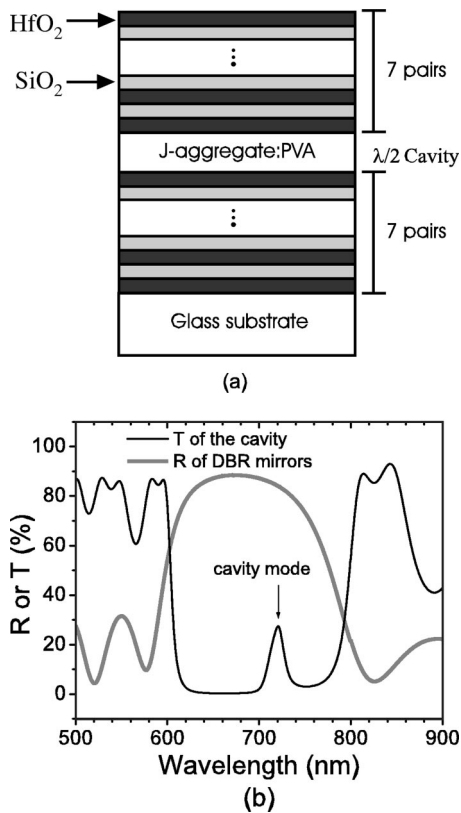


FIG. 1. (a) Schematic of the organic microcavity structure. Seven pairs of  $\text{HfO}_2$  ( $n=2.05$ ) and  $\text{SiO}_2$  ( $n=1.45$ ) quarter-wave layers were grown by reactive ion beam sputtering. (b) Normal incident reflectance of the DBR mirrors and transmittance of the microcavity structure.

simulation. We used DBRs of relatively low reflectivity in order to optimize one strong coupling condition, namely that the linewidth of the cavity mode should be matched to that of exciton resonance<sup>10</sup> while the reflection loss is less than absorption loss per pass.<sup>11</sup>

Figure 2 shows the microcavity transmission spectrum at

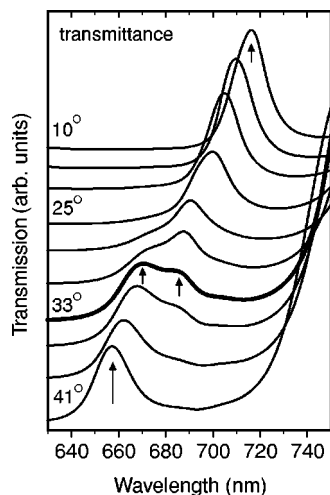


FIG. 2. Transmission spectrum of the microcavity at room temperature as a function of the external angle of incidence.

room temperature as a function of the external angle of incidence ( $\theta$ ). With increasing incident angle the cavity mode moves towards shorter wavelengths. When the detuning between the bare cavity and exciton modes approaches zero ( $\theta \sim 33^\circ$ ), normal mode splitting is observable with a Rabi splitting of 40 meV. This is smaller than previously reported values in a metal-DBR hybrid cavity (80 meV)<sup>12</sup> and in an all-metal cavity (300 meV)<sup>13</sup> with the same organic material, and is partly due to use of dielectric DBRs resulting in longer effective cavity length ( $L_{\text{eff}}$ ) than for metal mirrors (note that the Rabi splitting is proportional to  $(\alpha/L_{\text{eff}})^{1/2}$ , where  $\alpha$  is the peak absorption coefficient<sup>6,12</sup>). In our all-dielectric DBR cavity,  $L_{\text{eff}}$  is calculated to be  $1.40 \mu\text{m}$ ,<sup>14</sup> which is about 1.9 times longer than the metal-DBR hybrid cavity in Ref. 12. The further reduction in the Rabi splitting is attributed to smaller absorption coefficient of the J-aggregate layer, resulting from smaller dye concentration. For the purposes of optical switching applications in the strongly coupled regime, however, this splitting is more than adequate and enjoys the benefit of a vastly improved optical access into the transparent microcavity.

We have investigated the nonlinear response and the dynamics of the cavity polariton, by performing angle resolved pump-probe experiments on the microcavity structure. The optical source was a modelocked, amplified Ti:sapphire laser system with an optical parameter amplifier (OPA) that generated 100 fsec pulses at 125 kHz repetition rate at an average power of 1 mW. The output wavelength of OPA was tuned to 682 nm and, as the spectral width of the laser beam was 50 nm wide, we could pump the cavity polaritons resonantly at a fixed angle of incidence while covering the equivalent range of detuning from  $\theta=27^\circ$  to  $41^\circ$  in the external incident angle of the probe. A 25 nm-width, 680 nm bandpass filter was used for the quasi-monochromatic probe beam that was cross-polarized to the pump beam. The sample was mounted on a rotational stage to tune the cavity mode by varying the incident angle of the probe beam. The angle between the pump and the probe beam was kept  $45^\circ$ , so that change in the incident angle of the pump beam from  $18^\circ$  to  $4^\circ$  corresponded to a change in the probe beam angle from  $27^\circ$  to  $41^\circ$ . The pump intensity inside the cavity as a function of the incident angle was calculated by a standard transfer matrix simulation. Normalized to the intensity outside the sample, the intensity inside the microcavity was 0.027 at  $27^\circ$  of the probe angle ( $18^\circ$  of the pump angle), and monotonously decreased to 0.018 at  $41^\circ$ . The probe energy density was kept three order of magnitude smaller than pump pulse power to avoid any nonlinear effect by probe beam. All the experiments were carried out in transmission geometry at room temperature, with pump pulse energy density of the OPA output  $\sim 0.4 \text{ pJ}/\mu\text{m}^2$ .

As an example of our results, the transient modulated transmission  $\Delta T(t)/T$  of the bare exciton J-aggregate film (without cavity) and the cavity polariton (at the “strong coupling angle” of  $\theta=33^\circ$  of the probe) are compared in Fig. 3. Note that the weaker signal from the bare thin film is multiplied by a factor of ten. Simple exponential decays were used to fit the experimental data, showing that the relaxation process of the bare exciton has a fast component  $\tau_F=720$  fsec

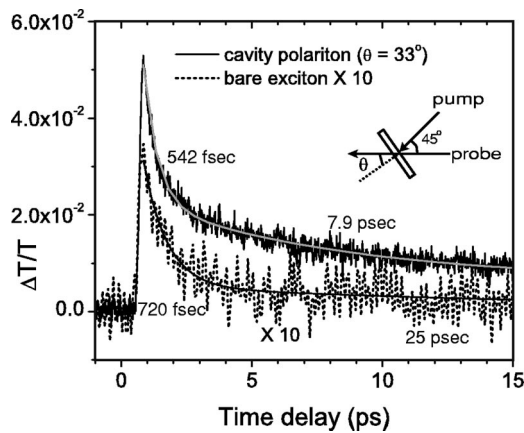


FIG. 3. Transient transmission spectrum of the cavity polariton at an angle  $\theta = 33^\circ$  (solid line) compared with bare thin film exciton (dotted line, note  $\times 10$  multiplication factor). The decay was fitted by two exponentials in each case. A schematic of pump-probe geometry is shown in the inset.

and a slow component  $\tau_S = 25$  psec, while the corresponding time constants are  $\tau_F = 542$  fsec and  $\tau_S = 7.9$  psec for the microcavity. For the thin film case, similar results have been reported on J-aggregates of squarylium dye<sup>9</sup> and pseudoisocyanine dye<sup>15</sup> thin films (no microcavity present), where the fast component and the slow component were attributed to a response induced by nonlinear electronic polarization of the J-aggregates and a population decay of the excited states to the ground state by collective superradiant emission, respectively. Even with the additional reflection losses in the microcavity sample (for coupling of pump excitation), more than one order of magnitude enhancement of the optical nonlinearity ( $\Delta T/T \sim 5\%$ ) is observed for the cavity polariton at the incident angle for the strongest coupling. In analog to the theoretical prediction of enhancement of nonlinearity due to microcavity effect for II-VI materials,<sup>16</sup> we attribute the effect to an electromagnetic enhancement in the coherency of the excitonic states. The case of J-aggregates is more complicated since, whereas the Frenkel excitons possess a very large oscillator strength, the medium is inherently disordered (orientational and density disorder), a fact that restricts the phase space where extended polariton states are well defined.<sup>17</sup> The states with the well-defined wave vector exist around zero detuning region of the wave vectors only;  $q_{\min}^{(L)} < q < q_{\max}^{(L)}$  for the lower branch, and  $q > q_{\min}^{(U)}$  for the upper branch. For the pumping mechanism, as stated in Ref. 17, the pump beam excites dispersionless incoherent states ( $q < q_{\min}^U$ ), which are similar to molecular excitation in the noncavity material, in our pumping configuration. Following the scenario in Ref. 17, the re-emission from these incoherent states pumps the cavity polariton states which set the coherence and the population. And then the coherence and the population are monitored by the probe beam in the coherent regime, i.e.,  $q_{\min}^U < q < q_{\max}^L$  in order to observe the strong coupling effect. Within this region of  $q$ , a coherent polarization can be created by the interplay of the photons and the ensemble of extended molecular resonances, leading to collective many-body states that possess a macroscopic transition dipole moment and enhanced nonlinear response

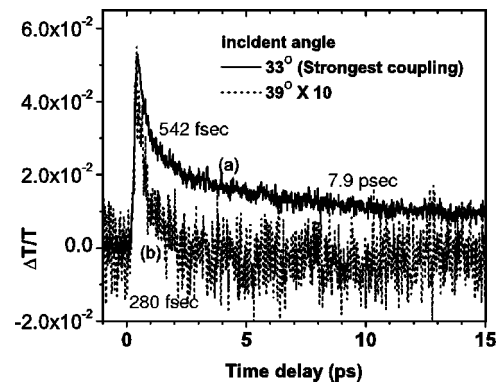


FIG. 4. Dependence of the exciton-photon coupling on the relaxation dynamics and the magnitude of the optical nonlinearity. The solid line (a) and dotted (b) lines represent the transient transmission at  $\theta = 33^\circ$  and at  $\theta = 39^\circ$ , respectively (note the  $10\times$  multiplication factor for the latter).

of the fast component. The population decay process for the slow component should be quite different in the polaritonic coherent region from the bare exciton. We speculate that the slow component (7.9 psec) reflect the interbranch transfer from the upper to lower branch (both are coherent states) around zero detuning region with the emission of a phonon. The interbranch decay time has been calculated to be approximately 10 psec.<sup>18</sup> We assumed that the decay from the lower branch to the ground state is significantly faster than the interbranch transition through coupled vibrational states.

As shown in Fig. 3, the fast components of the cavity polariton relaxation under the strong(est) coupling are more rapid than those of the bare exciton. Considering the relaxation dynamics mirrored by the fast component, we note that the photon lifetime in the empty microcavity is calculated to be  $\tau_C \sim 92$  fsec. To understand better the relationship between the degree of the exciton-photon coupling and its nonlinear dynamics, we performed probe-angle dependent experiments around zero detuning angle. Figure 4 shows an example where we compare the transient modulated transmission at resonance case [probe at  $\theta = 33^\circ$  (a)] with off-resonance case [ $\theta = 39^\circ$  (b)]. The amplitude of  $\Delta T/T$  at resonance is one order of magnitude larger than that for probe at  $\theta = 39^\circ$  and the relaxation times show a pronounced difference as well, these results being quite reproducible over several experiments. These experiments are summarized in Fig. 5, with (a) displaying the angular dependence of  $\Delta T/T$  (at zero pump-probe time delay) in relation to the polariton dispersion curve, while the normalized pump intensity was calculated to change monotonically from 0.022 (at  $31^\circ$ ) to 0.019 (at  $39^\circ$ ), demonstrating that simple passive resonator effects cannot be responsible for observed enhancement effects. Note how near the resonance,  $\Delta T/T$  changes by a factor of 3 with only a  $1^\circ$  change in the external incident angle of the probe beam, and that its maximum value occurs at the strongest coupling, emphasizing the enhancement of optical nonlinearity by polaritonic phenomena. Such a sharp angular dependence shows that the nonlinear enhancement is super-linear to the degree of coupling, which makes both an enhancement of coherency of the states and an appearance of excitonic component at the resonant angle.

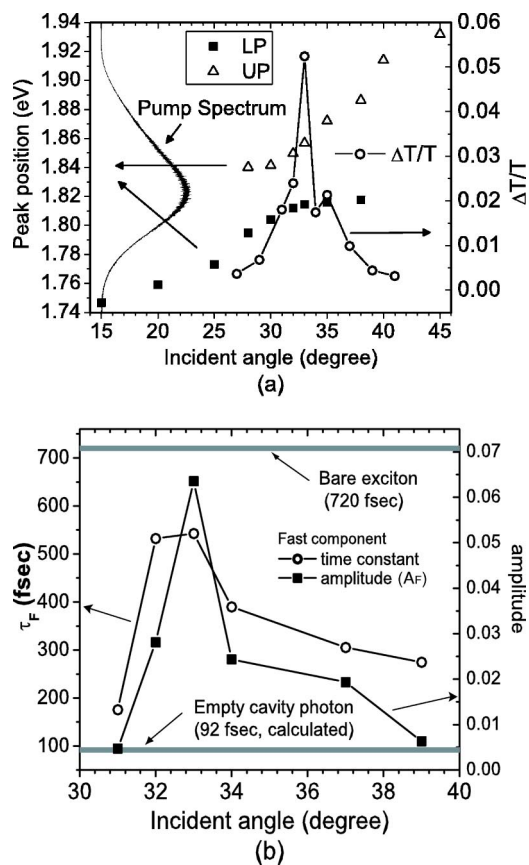


FIG. 5. (a) Upper (open triangles) and lower (solid squares) polariton dispersion curve and the magnitude of  $\Delta T/T$  (open circles) as a function of incident angle. The pump spectrum is included (solid line). (b) Variation of the fast relaxation component of the cavity polariton near the resonance angle. The time constants,  $\tau_F$  (open circles), and amplitudes,  $A_F$  (solid squares) are obtained by fitting the experimental data to  $\Delta T/T = A_F \text{Exp}(-t/\tau_F) + A_S \text{Exp}(-t/\tau_S)$ . The relaxation time of bare thin film exciton and photon life time of empty cavity are shown for reference.

The dynamics of  $\Delta T/T$ , specifically in terms of the relaxation times are also strongly dependent on the degree of exciton-photon coupling in our microcavity structures. The variation of the fast (coherent polarization dominated) decay component  $\tau_F$  as a function of incident probe angle is shown

in Fig. 5(b) (open circles); note how this cavity-polariton relaxation time is bracketed by that of bare exciton ( $\tau_F = 720$  fsec) and the photon lifetime of the empty cavity. Considering that the spectral widths of both the bare exciton and the cavity mode are relatively broad (20 nm each) in our structure, a spectral sum of the polariton states is expected to be probed in the transmitted light. In the absence of coupling (at off-resonant angle), the photon-like mode provides the means of excitation transfer out of the cavity. With increasing coupling, we begin to observe the contribution of the excitonic content to the polariton, which is the source of the optical nonlinearity. The excitonic admixture begins to dominate the relaxation dynamics, so the relaxation times become longer at the resonance, yet remain shorter than those of bare exciton due to the photonic admixture to the quasiparticle.

Finally, we comment on the “disappearance” of the slow component at off-resonant probe angles. The disappearance is more distinct at larger angles ( $q_0 < q$ , where  $q_0$  is the wave vector at zero detuning) while the slow component still remains detectable at shorter angle side up to  $29^\circ$  (not shown). Qualitatively, as the upper branch cannot be excited at larger angles where the energy difference between the upper branch and the center energy of the pump light becomes larger than the half width of the pump light, the interbranch population decay is expected to be suppressed. On the other hand, the excited states at shorter angles become incoherent states, when  $q < q_{\min}^{(U)}$ , that is not coupled to the cavity photon anymore. Since  $q_0$  is distinctly closer to  $q_{\min}^{(U)}$  than  $q_{\max}^{(L)}$  and  $q_{\min}^{(L)}$ ,<sup>17</sup> the probed excited states become incoherent more rapidly at shorter angles. This interpretation consistently explains the rapid amplitude decrease of fast component [Fig. 5(b), solid squares], and long-lived slow component in the shorter angle side, since no macroscopic dipole moment is induced in incoherent states and incoherent states should follow the dynamics of the bare (localized) exciton. The combination of large Frenkel exciton oscillator strength, the large dipole moment of a J-aggregate, the large exciton-intramolecular phonon interaction, and the optical microcavity creates a new physical situation not encountered in inorganic semiconductor microcavities, especially for polariton dynamics. Further work to test these ideas is under progress.

Research supported by the Defense Advanced Research Projects Agency and the National Science Foundation.

\*Fax (401) 863-1387. Electronic address: Jung-Hoon\_Song@Brown.edu

<sup>1</sup>Y. Yamamoto, *Nature (London)* **405**, 629 (2000).  
<sup>2</sup>H. Ishihara and K. Cho, *Appl. Phys. Lett.* **73**, 1478 (1998).  
<sup>3</sup>E. Hanamura, *Phys. Rev. B* **38**, 1228 (1988).  
<sup>4</sup>H. Wang, J. Shah, T. C. Damen, W. Y. Jan, E. Cunningham, M. Hong, and J. P. Mannaerts, *Phys. Rev. B* **51**, 14713 (1995).  
<sup>5</sup>M. Saba, C. Ciuti, J. Bloch, V. Thierry-Mieg, R. Andre, Le Si Dang, S. Kundermann, A. Mura, G. Bongiovanni, J. L. Staehli, and B. Deveaud, *Nature (London)* **414**, 731 (2001).  
<sup>6</sup>P. Kelkar, V. Kozlov, H. Jeon, A. V. Nurmikko, C.-C. Chu, D. C.

Grillo, J. Han, C. G. Hua, and R. L. Gunshor, *Phys. Rev. B* **52**, R5491 (1995).

<sup>7</sup>D. G. Lidzey, D. D. C. Bradley, M. S. Skolnick, T. Virgili, S. Walker, and D. M. Whittaker, *Nature (London)* **395**, 53 (1998).  
<sup>8</sup>D. G. Lidzey, D. D. C. Bradley, A. Armitage, Steve Walker, and M. S. Skolnick, *Science* **288**, 1620, (2000).  
<sup>9</sup>M. Furuki, M. Tian, Y. Sato, L. S. Pu, H. Kawashima, S. Tatsuura, and Osamu Wada, *Appl. Phys. Lett.* **78**, 2634 (2001).  
<sup>10</sup>P. V. Kelkar, V. G. Kozlov, A. V. Nurmikko, C.-C. Chu, J. Han, and R. L. Gunshor, *Phys. Rev. B* **56**, 7564 (1997).  
<sup>11</sup>C. Weisbuch, M. Nishioka, A. Ishikawa, and Y. Arakawa, *Phys.*

- Rev. Lett. **69**, 3314 (1992).
- <sup>12</sup>D. G. Lidzey, D. D. C. Bradley, T. Virgili, A. Armitage, M. S. Skolnick, and S. Walker, Phys. Rev. Lett. **82**, 3316 (1999).
- <sup>13</sup>P. A. Hobson, W. L. Barnes, D. G. Lidzey, G. A. Gehring, D. M. Whittaker, M. S. Skolnick, and S. Walker, Appl. Phys. Lett. **81**, 3519 (2002).
- <sup>14</sup>V. Savona, L. C. Andreani, P. Schwendimann, and A. Quattropani, Solid State Commun. **93**, 733 (1995).
- <sup>15</sup>M. L. Horng and E. L. Quitevis, J. Phys. Chem. **97**, 12408 (1993).
- <sup>16</sup>H. Ishihara and K. Cho, Appl. Phys. Lett. **71**, 3036 (1997).
- <sup>17</sup>V. M. Agranovich, M. Litinskaia, and D. G. Lidzey, Phys. Rev. B **67**, 085311 (2003).
- <sup>18</sup>V. Agranovich, H. Benisty, and C. Weisbuch, Solid State Commun. **102**, 631 (1997).